

Modelling of Combined Reinforcement of Ceramic Composites by Whisker and Transformation Toughening

G. M. Song, Y. Zhou, Y. Sun & T. C. Lei

School of Materials Science and Engineering, PO Box 433, Harbin Institute of Technology, Harbin 150001, People's Republic of China

(Received 10 April 1997; accepted 30 May 1997)

Abstract: An appropriate model of combine toughening in ceramic composites toughened with whiskers and transformation particles is presented to identify the effects of whisker toughening and transformation toughening. Whisker toughening includes whisker bridging and crack deflection. For transformation toughening, the shear effect is considered by using a shear factor, f , based on the dilatation contribution. Calculated results show that there are interactions among whisker bridging, crack deflection and transformation toughening. Crack bridging and crack deflection give rise to the contribution of transformation toughening, but transformation toughening produces a reduce to the contributions of whisker bridging and crack deflection. Predictions of the toughness of $\text{SiC}_w/\text{ZrO}_2(2\text{mol}\%\text{Y}_2\text{O}_3)/\text{Al}_2\text{O}_3$ based on the present model are showed to be in good agreement with the experimental results. © 1998 Elsevier Science Limited and Techna S.r.l.

1 INTRODUCTION

Whisker is found to be effective in strengthening and toughening ceramic materials,^{1–3} and the toughening is realised by main three toughening mechanisms, whisker bridging, whisker pullout and crack deflection.³ On the other hand, toughness has been improved remarkably by ZrO_2 t - m transformation in many ceramics.^{4–6} Toughness values can further be increased when both whiskers and particles are incorporated into ceramic matrix. In some cases, synergistic toughening has been observed and utilized.^{7,8} In the combine toughened ceramics with both SiC whiskers and ZrO_2 transformation particles, there are various toughening mechanisms that operate simultaneously, including whisker bridging, crack deflection, whisker pullout, microcracking and transformation, etc., during crack propagating. It is very difficult to identify experimentally the relative contribution and the role of each toughening mechanism. So theoretical modelling of combine toughening in ceramics toughened by multiple toughening methods is a long standing subject.

Several theoretical analyses of fibre bridging in fibre-reinforced ceramics has been proposed.^{9,10} A continuum model is introduced by Budiansky *et al.*¹¹ for an elastic solid which contains particles that undergo an irreversible stress-induce dilatation transformation. A model which includes both shear and dilatation effects of transformation toughening, has also been established,¹² which is perhaps more realistic than the early model which considers dilatation only. Amazigo *et al.*¹³ also presented a analysis model of synergistic toughening including crack bridging by ductile particles and dilatation transformation of ZrO_2 particles.

Whisker is a kind of short fibre and its orientation in ceramic matrix is usually random, which is different to unidirectional aligned long fibre. Crack deflecting along whisker/matrix interfaces is very frequently observed. Addition of ZrO_2 transformation particles in whisker-toughened ceramics makes toughening analysis more complicated. To date, there is not a suitable model to discuss this problem of combine toughening with both whiskers and ZrO_2 transformation particles.

Our previous experimental investigations on SiC whisker-ZrO₂ toughened Al₂O₃ ceramics^{7,8} show that whisker bridging, crack deflection and transformation are the main toughening mechanisms in these composites. In this paper, we try to provide a simple model of combine toughening, including whisker bridging, crack deflection and transformation, to analyse quantitatively combine toughening of whiskers and transformation particles, and the validity of this model is also identified by using some experimental results.

2 THEORETICAL MODEL

2.1 Whisker toughening

When a crack meets with a incline whisker, the whisker/matrix interface usually debonds and the whisker slips over a certain distance, L_s (Fig. 1). Assuming the incline whisker is not bending during the crack face opening process, the relation between the axial stress and the axial extension of the whisker into the crack face can be obtained according to the shear-lag model.⁹

$$\sigma_\phi = 2[E_w\tau(1 + \eta)/r_w]^{1/2}\sqrt{u_\phi} \quad (1)$$

where $\eta = E_w V_w / (E_m V_m)$, E_w and r_w are the Young's modulus and the radius of the whisker, respectively, and τ is the whisker/matrix interfacial shear stress¹⁴

$$\tau = \mu\Delta\alpha\Delta T / [(1 + \nu_m)/2E_m + (1 - 2\nu_w)/E_w] \quad (2)$$

where μ is the interfacial friction coefficient, $\Delta\alpha$ is the coefficient differential of thermal expansion, ΔT is the temperature differential between the temperature below which stress relaxation cannot take place and the temperature under consideration, and ν is Poisson's ratio.

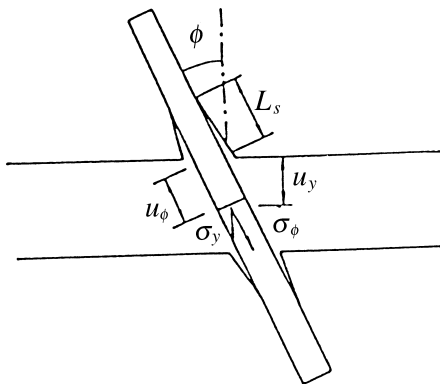


Fig. 1. An incline whisker bridging a crack.

Due to the geometric relation

$$\sigma_y = \sigma_\phi \cos^2 \phi \quad u_y = u_\phi \cos \phi \quad (3)$$

where σ_y is the crack cohesive stress from bridging whisker, u_y is the crack face opening distance. then

$$\sigma_y = 2 \cos^{3/2} \phi [E_w\tau(1 + \eta)/r_w]^{1/2} \sqrt{u_y} \quad (4)$$

For a single notch specimen (Fig. 2), the whisker bridging contribution is given by

$$\Delta K_b = \int_{a_0}^a \frac{2V_w\sigma_y(u_y(x))}{\sqrt{\pi a}} H(a/W, x/a) dx \quad (5)$$

where $H(a/W, x/a)$ is a weight function.¹⁵

In most whisker-reinforced ceramics, the crack deflection is usually observed, but the deflected distance along with whisker/matrix is often much less than the half length of whisker. The crack surface area is enlarged by crack deflection, so the toughening contribution associated with the crack surface area can be calculated. Assuming the maximum deflection length, L_d , equals the slipping distance, L_s , the resultant toughness from the additional surface area can be given by assuming that fracture surface morphology comprises cones (height, 0 to L_d)

$$y_d/y_m = \frac{2}{\pi} \frac{2}{\delta} \int_0^{\pi/2} \sqrt{\left(\frac{\delta}{2}\right)^2 + (L_s \sin \phi)^2} d\phi \quad (6)$$

where Y_d , Y_m are the strain energy release rates of deflected and undeflected crack, where δ is the centre to centre nearest neighbour spacing between whiskers.¹⁶ Equation (6) implies the influence of interface bonding strength effect on crack deflection through L_s . Then the crack deflection contribution is simply given by

$$\Delta K_d = (\sqrt{y_d/y_m} - 1) K_m \quad (7)$$

2.1.1 Transformation toughening

When a macroscopic crack propagates in a ceramic matrix containing ZrO₂ transformation particles.

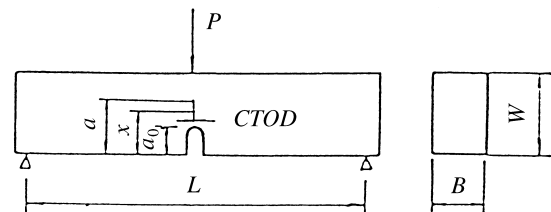


Fig. 2. A single-edged notch 3-point bending specimen.

The ZrO_2 in the vicinity of the crack tip will take place $t\text{-}m$ transformation and a transformation zone is formed (Fig. 3). It is assumed that the transformation zone is comprised of a continuum of dilation particles near crack tip. The hydrostatic stress, $\Sigma_m (= \frac{1}{3} \Sigma_{ii}, i = 1, 2, 3)$, applied on each dilation particle is given by

$$\Sigma_m = \frac{2(1+\nu)}{3} \frac{K_p}{\sqrt{2\pi r}} \cos(\theta/2) \quad (8)$$

where K_p is the elastic intensity factor determined for the actual geometry of a cracked specimen at a given load P , r and θ are the position co-ordinates of an expansion center relative to the crack tip, ν is Poisson's ratio.

If Σ_m reaches a critical value, σ_c , $t\text{-}m$ transformation will occur including a dilation of about 4% and a shear distortion of about 7%.⁶ A uniform dilation transformation of a ZrO_2 particle will produce a reduction in near crack-tip intensity relative to the applied intensity, and the stress intensity factor induced is

$$\Delta k = [G \cos(3\theta/2)] / [(2\pi)^{1/2} r^{3/2}] dA \quad (9)$$

where G is the shear modulus and dA is the volume dilation strain of each ZrO_2 particle.

A shear strain, ε^s , and dilation, ε^T , take place simultaneously during a ZrO_2 particle transforming, and the toughening contribution of the shear strain is of the same order of magnitude as that of the volume dilation.¹² To simplify the calculation of the contribution from transformation toughening, we presume a shear strain factor, f , which reflects the effect of shear strain. So the transformation effect from both shear strain and dilation strain can be obtained by

$$\Delta K_s = V_{t-m} G (f+1) \varepsilon^T \iint [\cos(3\theta/2)] / \left[(2\pi)^{1/2} r^{3/2} \right] r dr d\theta \quad (10)$$

where A denotes the region of the transformation zone, $(1+f)$ is assumed to represent shear strain and dilation, and V_{t-m} is the volume fraction of the ZrO_2 which takes place $t\text{-}m$ transformed in the total ZrO_2 .

2.1.2 Fracture resistance equation

For the notch specimen, the initial notch length, a_0 , is much longer than the crack growing length, $\Delta a (= a - a_0)$, until the instable propagation of the

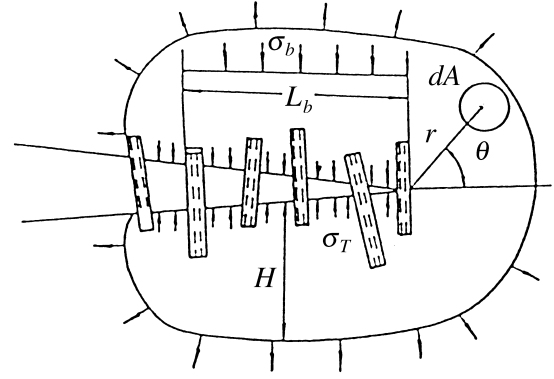


Fig. 3. Schematic of combine toughening of whisker and transformation.

crack. We still assume that the whole crack is a mode I crack, although the crack is deflected in the vicinity of the crack tip. As α is the angle between the crack faces, the crack opening displacement, $2u_y(x)$, at point x is

$$2u_y = \alpha(a - x) \quad (a_0 \leq x \leq a) \quad (11)$$

then the crack tip opening displacement $CTOD$ is

$$CTOD = \alpha(a - a_0) \quad (12)$$

When $u(x) \geq u_{yc}$ ($2u_{yc}$ is the critical opening displacement of the crack face), the whisker at point x will break and the crack closure stress $\sigma_y(x) V_w = 0_o$.

The stress intensity factor K_p due to the external load P is

$$K_p = \frac{3PL}{2BW^2} \sqrt{a} F(a/W) \quad (13)$$

where $F(a/W)$ is a weight function.¹⁵

As a crack propagates, the fracture resistance K_r is

$$K_r = K_m + \Delta K_s + \Delta K_b + \Delta K_d \quad (14)$$

where K_m is the fracture toughness of the matrix, and ΔK_s , ΔK_b and ΔK_d are the contributions of transformation, whisker bridging and crack deflection, respectively. Equation (14) includes three toughening mechanisms, transformation, whisker bridging and crack deflection.

3 EXPERIMENTAL PROCEDURE

Al_2O_3 powder with a average size of about $0.1 \mu\text{m}$ is used as the basic material. ZrO_2 powder stabilised by 2mol% Y_2O_3 and SiC whisker was prepared as

reinforcements. According to the proportion of $\text{Al}_2\text{O}_3 + (10, 20, 30 \text{ vol}\%) \text{ZrO}_2 + (10, 20, 30 \text{ vol}\%) \text{SiC}_w$, these powders and whiskers are mixed by ball milling for 24 h in an hydrous alcohol. the mixtures are dried and green-compacted at 250 MPa and then hot pressed at 1650°C, 25 MPa for 45 min. The temperature lies for hot pressing in the single tetragonal phase region of $\text{ZrO}_2\text{-Y}_2\text{O}_3$ diagram. The fracture toughness is measured with an Instron-1186 testing machine using the single-edge notch 3-point bend specimen, $30 \times 4 \times 2$, with a notch depth, 2 mm. The volume percentage of $t\text{-ZrO}_2$ in total ZrO_2 is measured with X-ray diffraction (XRD) on the as-polished and the fracture surfaces.

4 RESULTS AND DISCUSSION

These parameters of $\text{SiC}_w/\text{ZrO}_2(2\text{mol}\%\text{Y}_2\text{O}_3)/\text{Al}_2\text{O}_3$ ceramics are used to calculate the fracture curves, $E_{\text{SiC}_w} = 550 \text{ GPa}$, $E_{\text{Al}_2\text{O}_3} = 400 \text{ GPa}$, $E_{\text{ZrO}_2} = 220 \text{ GPa}$, $\varepsilon^T = 5\%$, $f = 0.8$, $\sigma_c = 700 \text{ MPa}$. The X-ray diffraction patterns show that about 20 vol% tetragonal ZrO_2 has transformed into monoclinic ZrO_2 in total ZrO_2 particles during the fracture process of the composites. Thereby $V_{t-m} = 0.2$. The fracture toughness of Al_2O_3 is $K_{\text{Al}_2\text{O}_3} = 4.4 \text{ MPam}^{1/2}$, and fracture toughness of ZrO_2 which did not transform is $K_{\text{ZrO}_2} = 3.4 \text{ MPam}^{1/2}$. For the whisker, $\sigma_w = 8 \text{ GPa}$, $r_w = 0.5 \mu\text{m}$, and whisker length $L = 25 \mu\text{m}$. The friction coefficient of whisker/matrix (matrix consists of Al_2O_3 and ZrO_2 which did not transform) interface is $\mu = 0.4$. For the specimen, $a_0 = 2.5 \text{ mm}$, $W = 5 \text{ mm}$, $B = 2.5 \text{ mm}$, and the span $L = 20 \text{ mm}$.

Applying external stress intensity K_p , and then P can be given by eqn (13). Calculating K_r , if $K_p < K_r$, K_p increases. When $K_r = K_p$, the main crack a is allowed to extend a small increment $da (= a_0/2000)$. At each increment in K_p and da , the calculations of K_r and P are repeated until the main crack propagates in a unstable manner, and then a crack resistance curve, or R-curve vs the crack growth length is obtained. At the point of maximum load, P_{max} , the fracture toughness, K_{IC} , and the corresponding contributions from transformation, whisker bridging and crack deflection, ΔK_{sc} , ΔK_{bc} and ΔK_{dc} can be obtained.

Figures 4 and 5 show the calculated R-curves for $\text{SiC}_w/\text{ZrO}_2(2\text{mol}\%\text{Y}_2\text{O}_3)/\text{Al}_2\text{O}_3$ composites with different whisker content (Fig. 4) or ZrO_2 content (Fig. 5). When the crack propagates initially, transformation, whisker bridging and crack deflection all take place in the vicinity of the crack tip, so ΔK_s , ΔK_b and ΔK_d increase, which results in a

rapid rise in fracture resistance, K_r . For further crack extension, a higher value of the applied K_p is required. With the further crack propagation, due to some whiskers which bridge the crack failing, a transformation wake zone is formed, the increase in ΔK_s and ΔK_b no longer rise remarkably, thereby the slope of R-curves gradually drops, and these curves will also tend to become parallel lines.

The effective fracture toughnesses calculated are shown in Tables 1 and 2. For the same ZrO_2 content, ΔK_s , ΔK_b and ΔK_d increase with increasing whisker content, as shown in Table 1, it implies that an increment in whisker content will give rise to each contribution of whisker bridging, crack deflection and transformation. With increasing whisker content, ΔK_b and ΔK_d will be increased, as suggested by eqns (5) and (6), which results in a rise in K_r . To drive the crack, K_p is needed to increase, leading to an enlargement of the transformation zone. So ΔK_s is increased. Whisker toughening is beneficial to transformation. In contrast, for the same whisker content, with increasing

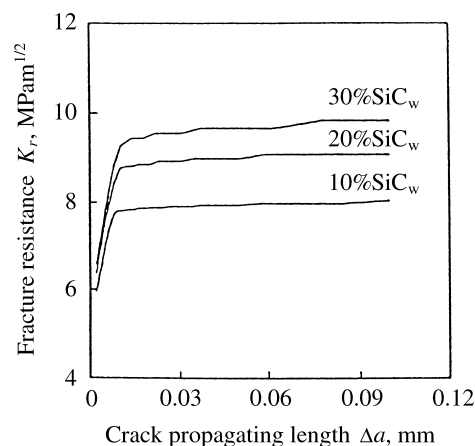


Fig. 4. R-curves vs whisker content in $\text{SiC}_w/20 \text{ vol}\%\text{ZrO}_2/\text{Al}_2\text{O}_3$ ceramics.

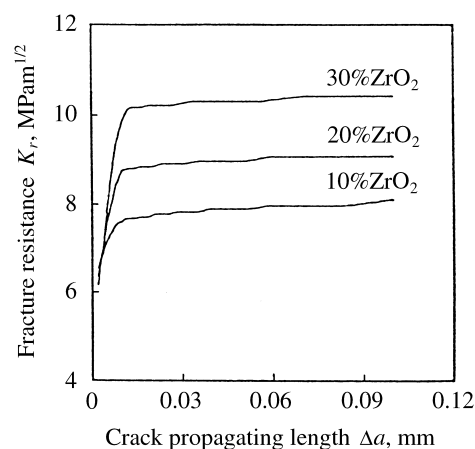


Fig. 5. R-curves vs ZrO_2 content in $20 \text{ vol}\%/\text{SiC}_w/\text{ZrO}_2/\text{Al}_2\text{O}_3$ ceramics.

Table 1. The toughness of SiC_w/20 vol%ZrO₂/Al₂O₃, MPa m^{1/2}

SiC _w (vol%)	Calculated				Measured
	ΔK_{sc}	ΔK_{bc}	ΔK_{dc}	K'_{IC}	
10	2.219	0.316	1.142	7.853	7.31
20	2.708	0.676	1.466	8.968	9.10
30	3.092	0.901	1.615	9.65	9.87

Table 2. The toughness of 20 vol%SiC_w/ZrO₂/Al₂O₃, MPa m^{1/2}

ZrO ₂ (vol%)	Calculated				Measured
	ΔK_{sc}	ΔK_{bc}	ΔK_{dc}	K'_{IC}	
10	1.151	0.800	1.558	7.898	7.85
20	2.708	0.676	1.66	8.968	9.10
30	4.50	0.486	1.383	10.22	10.38

ZrO₂ content, ΔK_s increases, but ΔK_b and ΔK_d all decrease. The rise of transformation particle content gives rise to ΔK_s . As a result of that, K_r is increased, and the external applied load K_p has to be increased for driving the crack which causes the crack face opening displacement to increase. Therefore some whiskers bridging the crack face will fail, and ΔK_b decreased. Because the crack deflection is only related to the whisker bridging, as suggested by crack deflection model (eqn (6)), ΔK_d is decreased when ΔK_b decreases. Thereby the exist of transformation particle is not beneficial to the toughening of whisker bridging or crack deflection.

5 SUMMARY

A analytical model of combine toughening in ceramics toughened with whiskers and transformation particles is proposed based on three toughening mechanisms, whisker bridging, crack deflection and transformation. It is used to estimate quantitatively their toughening contributions, and the calculated results of fracture toughness for SiC_w/ZrO₂(2mol%Y₂O₃)/Al₂O₃ ceramic composites show that the values of calculated toughness are in good agreement with that of experimental results. There is interaction between the transformation, whisker bridging and crack deflection. Whisker bridging and crack deflection prompt transformation toughening. In contrast, transformation toughening produces a reduction to the toughening effects of whisker bridging and crack deflection.

Transformation in ZrO₂ is accompanied by extensive microcracking although the effects of microcracking are thought of as small compared with that of transformation. And microcracking is also beneficial to crack deflection. These more complex toughening phenomena need further study.

REFERENCES

1. BECHER, P. F. & WEI, G. C., Toughening behavior in SiC whisker-reinforced alumina. *J. Am. Ceram. Soc.*, **67** (1984) C267.
2. FABER, K. T. & EVANS, A. G., Crack deflection Process-I. Theory. *Acta Metall.*, **31** (1983) 565–576.
3. BENGISU, M., INAL, O. T. & TOSYALI, O., On whisker toughening in ceramic materials. *Acta Metall. Mater.*, **39** (1991) 2509–2517.
4. EVANS, A. G. & CANNON, R. M., Toughening of brittle solids by martensitic transformations. *Acta Metall.*, **34**(5) (1986) 761–800.
5. EVANS, A. G. & HEUER, A. H., Review-Transformation toughening in ceramics: martensitic transformation in crack-tip stress fields. *J. Am. Ceram. Soc.*, **63**(5–6) (1980) 241–248.
6. ZHOU, Y., Microstructure and mechanical properties of ZrO₂-Y₂O₃ ceramics, Ph.D. thesis, Harbin Institute of Technology, Harbin, 1989 (in Chinese).
7. LIN, G. Y., LEI, T. C., ZHOU, Y. & WANG, S. X., Mechanical properties of Al₂O₃ and Al₂O₃+ZrO₂ ceramics reinforced by SiC whiskers. *J. Mater. Sci.*, **28** (1993) 2745–2749.
8. LEI, T. C., GE, Q. L., ZHOU, Y. & WANG, S. X., Microstructure and fracture behavior of an Al₂O₃-ZrO₂-SiC_w ceramic composite. *Ceram. Int.*, **20** (1994) 91–97.
9. MARSHALL, D. B., COX, B. N. & EVANS, A. G., The mechanics of matrix cracking in brittle-matrix fiber composites. *Acta Metall.*, **33** (1985) 2013–2021.
10. VICTOR, C. Li., JIANG, W. Y. & STANLEY, B., A micromechanical model of tension softening and bridging toughening of short random fiber reinforced brittle matrix composites. *J. Mech. Phys. Solids*, **39**(5) (1991) 607–625.
11. BUDIANSKY, B., HUTCHINSON, J. W. & LANBROPOLOUS, J. C., Continuum theory of transformation toughening in ceramics. *Int. J. Solids Struct.*, **19** (1983) 337–355.
12. CHEN, I. C. & MOREL, P. E. E., Implications of transformation plasticity in ZrO₂-containing ceramics: I, shear and dilatation effects. *J. Am. Ceram. Soc.*, **69**(3) (1986) 181–189.
13. AMAZIGO, J. C. & BUDIANSKY, B. J., Interaction of particulate and transformation toughening. *J. Mech. Phys. Solids*, **36** (1980) 581–595.
14. BECHER, P. F., TIEGS, T. N., OGLE, J. C. & WARWICK, W. H., Toughening of ceramics by whisker reinforcement. In *Fracture mechanics of Ceramics*, Vol. 7, ed. R. C. Bradt, A. G. Evans, D. P. Hasselman & F. F. Lange. Plenum Press, New York, 1986, pp. 639–649.
15. TADA, H., PARIS, P. C. & IRWIN, G. R., *The Stress Analysis of Cracks Handbook*. Del Research Corporation, Hellertown, Pa., 1973, pp. 2, 16–27.
16. BANSAL, P. P. & ARDELL, A. J., Average nearest-neighbor distances between uniformly distributed finite particles. *Metallography*, **5** (1972) 97–111.